



Influence of Injection Rate and Oil Viscosity on Viscous Fingering – Simulation Prediction

Abdul Afiq Abdul Aziz¹, Nadiahnor Md Yusop^{1,2,*}, Noraishah Othman³

¹ School of Chemical Engineering, College of Engineering, Universiti Teknologi MARA (UiTM) Shah Alam, Selangor, Malaysia

² Energy, Oil & Gas, Smart Manufacturing Research Institute (SMRI), Universiti Teknologi MARA (UiTM) Shah Alam, Malaysia

³ Malaysian Nuclear Agency, Malaysia

ARTICLE INFO

Article history:

Received 12 May 2022

Received in revised form 20 May 2022

Accepted 21 May 2022

Available online 7 June 2022

Keywords:

Waterflooding; injection rate; oil viscosity; viscous fingering

ABSTRACT

Waterflooding is a secondary oil recovery process that commonly utilized. However, there are several factors affecting the efficiency of water-flooding. Current research focused on the effects of injection rate and oil viscosity on the waterflooding efficiency. Fluid Structure Interaction (FSI) is utilized to predict the effect of the injection rate and oil viscosity towards waterflooding. Volume of fluid (VOF) and Realizable $k-\epsilon$ models are utilized in this research. Ergun's equation also utilized in this research for estimation of permeability and inertial loss within the porous medium. The research found viscous fingering occurred when the mobility ratio is more than unity and instability number, $N_i > 1000$. The phenomenon of viscous fingering is directly affected by injection rate and viscosity ratio. The phenomenon directly affects directly sweep efficiency during waterflooding process thus affecting oil recovery process. The research found as injection rate and viscosity ratio increase; viscous fingering predominantly seen within the porous medium.

1. Introduction

Enhanced oil recovery (EOR) is utilized to obtain significant reserve improvement in mature oil fields. Enhanced oil recovery (EOR) process is considered more feasible than accessing to new fields which more challenging and require significant upfront capital investment [1]. One of common enhanced oil recovery (EOR) method is waterflooding. Waterflooding is a secondary oil recovery method used to increase oil production from reservoir. The water sources that commonly utilized for the waterflooding process are seawater, freshwater, injecting water from other reservoirs or produced water; i.e., water that is separated from the oil and gas production facilities [3]. Waterflooding commonly applied for the light oil recovery. Therefore, seawater is commonly utilized for the waterflooding process due to its displacement, wide accessibility, and cheap [4]. Basic concept of water flooding utilizes water, where the water is displaced to create the formation of pressure maintenance within the reservoir. Waterflooding is mainly applied in the development of porous

* Corresponding author.

E-mail address: nadiahnor@uitm.edu.my (Nadiahnor Md Yusop)

<https://doi.org/10.37934/cfdl.14.6.2442>

reservoir. It is efficient for hydrophilic rock and homogeneous reservoir system [5]. The injected water displaces the oil and occupies the pore space [6].

Most reservoirs have anisotropic fluid flow due to their heterogeneity's structures. Hence, it is difficult to predict the fluid flow. Thus, the investigation on the hydrodynamics and behaviour of the reservoir during waterflooding has been performed by Dugstad *et al.*, [7]. He mentioned one of the difficulties in waterflooding operations is to quantify the oil production and the effect of waterflooding operations usually performed through pilot studies. Tracer is used to estimate the potential and effect of oil recovery method.

Adverse mobility ratio between crude oil and water causes fingering found within the reservoir for viscous oil. This phenomenon leaves large quantities of residual oil within the reservoir [8]. This phenomenon called viscous fingering where an instability under miscible or immiscible conditions occurs when less viscous injected fluid displaces a much more viscous resident fluid. It is difficult to simulate immiscible viscous fingering and a numerous of studies have applying high order numerical schemes to the immiscible viscous fingering problem with limited success [26].

The efficiency of waterflooding is highly dependent on the mobility ratio, M , as per Eq. (1). As mentioned by Palsson *et al.*, [9], water injection is considered successful when it can maximize the overall recovery. Apparently, the measurement of the oil recovery will be on the waterfront sweep distribution, accelerating hydrocarbon production, minimizing water production, and handling cost, and minimizing any environmental impacts.

$$M = \frac{\lambda_D}{\lambda_d} = 1 \quad (1)$$

where λ_D is mobility of displacing fluid (water/working agent) and λ_d is mobility of displaced fluid (oil). Perfect mobility ratio is unity. It is unfavourable for waterflooding when mobility ratio is greater than unity because viscous fingering likely to occur. Consequently, mobility ratio equal and less than unity is favourable for waterflooding. Kargozarfard *et al.*, [10] mentioned that the increase of mobility ratio causing oil recovery challenges more severe. Viscous fingering can reduce the sweep efficiency within the reservoir. Consequently, it can reduce the oil recovery.

Eq. (1) can be expanded with the relationship of viscosity and relative permeability [11]. The extended version of the Eq. (1) is written as;

$$M = \frac{\lambda_D}{\lambda_d} = \frac{k_{rw}/\mu_w}{k_{ro}/\mu_o} \quad (2)$$

where k_{rw} and k_{ro} is relative permeability of water and oil respectively and μ_w is viscosity of water (in centipoise) and μ_o is viscosity of oil (in centipoise). Eq. (2) illustrates the viscosity ratio is directly proportional to the mobility ratio. Thus, it can affect the oil displacement within the reservoir due to the viscous fingering phenomena.

In term of injection rate towards viscous fingering, Kargozarfard *et al.*, [10] conducted a study of two-phase fluid flow in porous medium. They observed both viscous forces and capillary forces compete in the medium for the oil displacement. The ratio of both these forces is known as capillary number. The viscous force dominates over the capillary force when capillary number is high. Therefore, viscous fingering occurred in the medium. Consequently, the sweep efficiency is reduced, and the phenomenon reduce the oil recovery. Kargozarfard *et al.*, [10] concluded viscosity and injection rate are the important parameter for oil recovery; both parameters can cause viscous fingering. The previous study done by Jin *et al.*, [18] concluded inconsistent with the capillary number theory where the result shows increasing injection rate causing oil recovery to decrease.

By being able to predict the occurrence of viscous fingering during waterflooding, it will be able to save time and cost during the waterflooding process and improve the performance of the waterflooding process by using proper process parameter. Thus, the objective of this study is to predict the hydrodynamics effect of the injection rate and viscosity ratio toward the occurrence of viscous fingering during waterflooding. In addition to the hydrodynamic effect, the paper concluded on the sweep efficiency which determine the performance of the waterflooding.

1.1 Sweep Efficiency

There are two types of sweep efficiency which are areal sweep efficiency and vertical sweep efficiency. The combination of both areal and vertical sweep efficiency will produce volumetric sweep efficiency. This volumetric sweep efficiency is important to evaluate the effectiveness of waterflooding. The volumetric sweep efficiency is affected by several parameters which are mobility ratio, gravitational and capillary force, rate of injection and reservoir heterogeneity [12]. The sweep efficiency can be calculated by using Eq. (3) suggested by Fu-qing and Zhen-quan [13] as below;

$$E_V = \frac{S_w - S_{wc}}{1 - S_{wc} - S_o} \quad (3)$$

where S_w is average saturation in column, S_{wc} is irreducible water saturation, and S_o is average oil saturation in swept zone.

Sweep efficiency is an important factor to determine whether the displacement of the residual oil is occurred or not. If the sweep efficiency for waterflooding is low, it means the injected water insufficient to displace the residual oil. Consequently, this affects the estimation of the oil recovery potential and production. Displacement efficiency also affects the sweep efficiency. Common practice on the analysis for the sweep efficiency determination involves laboratory test, reservoir engineering data, and numerical simulation. The disadvantages of laboratory test dealt with high cost, less efficient, and the core sample vaguely show the heterogeneity of the reservoir [14]. Foreseeing the outcome of the sweep efficiency study, it is expected to improve the waterflooding method.

The fluid properties within the reservoir have major effects on the suitability for waterflooding too. Crude oil viscosity is a paramount parameter determining the success of oil recovery using waterflooding. Oil viscosity can affect the mobility ratio which directly control the sweep efficiency [15]. Generally, the viscosity ratio between the displaced fluid to the displacing fluid affect the waterflood displacement or sweep efficiency. Therefore, viscosity ratio in oil recovery prediction is important [16].

Injection rate is also a parameter that could affect the sweep efficiency. Different reservoir characteristic can have different injection rate. Slow injection rate can increase of sweep for lower permeability layer. High injection rate gives faster recovery, consequently resulting in high pressures. The high pressure induces fracture and adversely affect sweep efficiency, consequently, affect the adjacent structures due to instabilities. Therefore, optimum injection strategy is required depending on the characteristic of reservoir [12].

1.2 Relative Permeability

Relative permeability is included in the mobility ratio calculation as described in Eq. (2). There is various method used to calculate relative permeability. These methods are Corey's relative permeability correlations, Pirson's relative permeability correlations, and Brooks-Corey relative

permeability correlations. The calculation of relative permeability is affected by the type of process of flooding which are either drainage or imbibition process in either water-wet or oil-wet system.

Drainage process is the displacement of wetting phase by a nonwetting phase causing the saturation of the nonwetting increases. Whereas, for imbibition process, the displacement of nonwetting saturation by wetting phase occurred causing the nonwetting saturation to decreases [17]. In water-wet system, the wetting phase is water and the nonwetting phase is oil. Meanwhile, in oil-wet system, the wetting phase is oil and the nonwetting phase is water. The types of systems can be determined by estimating the water saturation within the reservoir. As mentioned by Ahmed [15], for initial water saturation more than 50%, it is a water-wet system whereas for initial water saturation less than 50%, it is an oil-wet system.

For waterflooding, it is commonly an imbibition process where water is injected to displaces oil within the pore spaces. In this investigation, Pirson's relative permeability correlations for water-wet imbibition operation is chosen. The correlations can be calculated using Eq. (4) and Eq. (5) below;

$$k_{rw} = \sqrt{S_w^*} \cdot S_w^4 \quad (4)$$

$$k_{rnw} = \left[1 - \left(\frac{S_w - S_{wc}}{1 - S_{wc} - S_{nw}} \right) \right]^2 \quad (5)$$

Where S_{nw} is nonwetting phase saturation, S_w is water saturation, S_{wc} is connate (irreducible) water saturation, and S_w^* is effective water saturation where can be calculated using Eq. (6) below;

$$S_w^* = \frac{S_w - S_{wc}}{1 - S_{wc}} \quad (6)$$

1.3 Capillary Number and Instability Number

Capillary number is an important parameter to consider in oil recovery operation. It indicates the magnitude of viscous forces in relation to forces due to interfacial tension. The capillary number can be expressed as Eq. (7) below;

$$N_{CA} = \left(\frac{C k_w \Delta p}{\phi \sigma_{ow} L} \right) \quad (7)$$

where N_{CA} is capillary number, dimensionless; C is a constant; k_w is effective permeability to water; ϕ is rock porosity, fraction; σ_{ow} is interfacial tension between oil and water. Eq. (7) illustrates as capillary number increases, the interfacial tension between fluids in the rock pores decreases while the oil recovery is expected to be increased [11].

Based on study done by Mai and Kantzas [24], for heavy oil waterflooding, instability number is used to predict the waterflooding process. The instability number described in Eq. (8) [25];

$$N_i = \left(\frac{v_w \mu_w}{\sigma_{ow}} \right) \left(\frac{\mu_o}{\mu_w} \right)^2 \left(\frac{D^2}{K} \right) \quad (8)$$

Where σ_{ow} is interfacial tension, D is diameter of core and K is permeability. Eq. (8) incorporates viscosity ratio into capillary number which is main factor affecting sweep efficiency. For the range of $N_i < 13.56$, the displacement is stable. Meanwhile, for the $N_i \geq 1000$, the displacement is deemed fully

unstable that possible of single finger to dominates flow causing low recovery and relatively independent of injection rate [24].

Viscous fingering can affect sweep efficiency which one of the investigations to predict its effect towards the oil recovery rate. A study done by Suekane *et al.*, [19] showed that viscous fingering can reduce the displacement efficiency. They observed several factors viscous fingering occurred because of viscosity ratio, Péclet number, and gravity number.

2. Methodology

2.1 Numerical Methods

2.1.1 Mass, momentum, and energy conservation

A numerical simulation of Darcy scale for waterflooding in a packed sand column which acted as artificial oil reservoir has been performed. The fluid within the packed sand column is assumed incompressible. The mass conservation described by Eq. (9);

$$\frac{\partial \rho}{\partial t} + \nabla \cdot (\rho \vec{V}) = S_m \quad (9)$$

where ρ is density, t is time, V is velocity, and S_m is source term. The source term commonly used if there any accumulation or generation of mass. If there is no accumulation or generation of mass, the source term will be zero. Since this study is only to know the displacement of the oil which mass inlet is equal to mass outlet so there is no generation or accumulation occurred in this study. Thus, the accumulation or generation term is zero ($S_m=0$).

The momentum conservation equation described by Eq. (10);

$$\rho \left[\frac{\partial \vec{V}}{\partial t} + \vec{V} \cdot \nabla \vec{V} \right] = -\nabla p + \nabla \cdot \vec{\tau} + \rho g + \vec{F}_b \quad (10)$$

where;

$$\vec{V} \cdot \nabla \vec{V} = u \frac{\partial \vec{V}}{\partial x} + v \frac{\partial \vec{V}}{\partial y} + w \frac{\partial \vec{V}}{\partial z} \quad (11)$$

Where ρ is density, t is time, V is velocity, p is pressure, μ is viscosity, F_b is body forces, u , v , and w are velocity component for x , y , and z direction respectively, and τ is shear stress tensor. In porous medium, the momentum conversation is modelled by addition of a momentum source term (S_i) where Eq. (10) is expanded into Eq. (12);

$$\rho \left[\frac{\partial \vec{V}}{\partial t} + \vec{V} \cdot \nabla \vec{V} \right] = -\nabla p + \nabla \cdot \vec{\tau} + \rho g + S_i \quad (12)$$

$$S_i = - \left(\frac{\mu}{\alpha} v_i + C_2 \frac{1}{2} \rho |v| v_j \right) \quad (13)$$

Where α is permeability, and C_2 is inertial loss coefficient.

The energy equation in porous medium is described in Eq. (14);

$$\frac{\partial (\gamma \rho_f E_f + (1-\gamma) \rho_s E_s)}{\partial t} + \nabla \cdot [\vec{v} (\rho_f E_f + p)] = \nabla \cdot [k_{eff} \nabla T - (\sum_i h_{ij} j_i) + (\vec{\tau} \cdot \vec{v})] + S_f^h \quad (14)$$

In this investigation, isothermal environment is considered where both fluid and solid have no temperature changes. Thus, there is no enthalpy energy for both fluid and solid. Therefore, only potential energy of the fluid is available with no generation of energy ($S_f^h=0$) thus Eq. (14) is simplified into Eq. (15);

$$\frac{\partial(\gamma\rho_f E_f)}{\partial t} + \nabla \cdot [\vec{v}(\rho_f E_f + p)] = \nabla \cdot [(\vec{\tau} \cdot \vec{v})] \quad (15)$$

Where γ is porosity, ρ_f is density, E_f is total fluid energy, t is time, v is velocity, p is pressure, τ is shear stress tensor. The total fluid energy, E_f , is

$$E_f = -\frac{p}{\rho_f} + \frac{v^2}{2} \quad (16)$$

2.1.2 Multiphase volume of fluid (VOF) model

Volume of Fluid (VOF) multiphase modelling is utilized to investigate the interaction between two immiscible fluids i.e oil and water. The model solved the mass fraction of each element within each phase. VOF model basically derived based Eq. (4) which is the conservation of mass. Eq. (17) below showed the VOF model;

$$\frac{1}{\rho_q} \left[\frac{\partial}{\partial t} (\alpha_q \rho_q) + \nabla \cdot (\alpha_q \rho_q \vec{v}_q) \right] = S_{\alpha_q} + \sum_{p=1}^n (\dot{m}_{pq} - \dot{m}_{qp}) \quad (17)$$

Where α_q is volume fraction of phase q , ρ_q is density for phase q , m_{qp} is the mass transfer from phase q to phase p and m_{pq} is the mass transfer from phase p to phase q , and S_{α_q} , is source term. This model also suitable for control volumes that filled with either a single or more fluid phases which like the condition within porous medium.

2.1.3 Ergun's equation for porous medium

In this investigation, packed sand column is assumed to be porous medium. The porous medium is commonly known as solid matrix containing fluid filled pores. Since fluid able to flow through the pores, porous medium also considered as rigid and open cell saturated because the pores are connected and filled with fluid completely [2]. Ergun equation is used to determine the viscous and inertial resistance within the porous media since the porous media is assumed to be homogenous packed bed of sand. The Ergun equation is described as per Eq. (18) below;

$$\frac{|\Delta p|}{L} = \left(\frac{150\mu}{D_p^2} \cdot \frac{(1-\varepsilon)^2}{\varepsilon^3} \cdot v_\infty \right) + \left(\frac{1.75p}{D_p} \cdot \frac{(1-\varepsilon)}{\varepsilon^3} \cdot v_\infty^2 \right) \quad (18)$$

where μ is the viscosity, D_p is the mean particle diameter, L is the bed depth, and ε is the porosity. By comparing with Eq. (18) with Eq. (13), the permeability, α , and inertial loss coefficient, C_2 , for each axis direction are determined using Eq. (19) and Eq. (20);

$$\alpha = \frac{D_p^2 \varepsilon^3}{150 (1-\varepsilon)^2} \quad (19)$$

$$C_2 = \frac{3.5(1-\varepsilon)}{D_p \varepsilon^3} \quad (20)$$

2.1.4 Turbulence realizable $k-\varepsilon$ model

Realizable $k-\varepsilon$ model written in Eq. (21) and Eq. (22) are utilized for the hydrodynamic investigation within the porous medium. The model transport is based on the turbulence kinetic energy (k) and its dissipation rate (ε).

$$\frac{\partial}{\partial t}(\rho k) + \frac{\partial}{\partial x_j}(\rho k u_j) = \frac{\partial}{\partial x_j} \left[\left(\mu + \frac{\mu_t}{\sigma_k} \right) \frac{\partial k}{\partial x_j} \right] + G_k + G_b - \rho \varepsilon - Y_M + S_k \quad (21)$$

$$\frac{\partial}{\partial t}(\rho \varepsilon) + \frac{\partial}{\partial x_j}(\rho \varepsilon u_j) = \frac{\partial}{\partial x_j} \left[\left(\mu + \frac{\mu_t}{\sigma_\varepsilon} \right) \frac{\partial \varepsilon}{\partial x_j} \right] + \rho C_{1\varepsilon} S_\varepsilon - \rho C_{2\varepsilon} \frac{\varepsilon^2}{k + \sqrt{\nu \varepsilon}} + C_{1\varepsilon} \frac{\varepsilon}{k} C_{3\varepsilon} G_b + S_\varepsilon \quad (22)$$

where ρ is density, t is time, u_j is Cartesian velocity component, μ is viscosity, μ_t is turbulence viscosity, ν is kinematic viscosity, σ_k and σ_ε are turbulence Prandtl number for k and ε respectively, G_k and G_b are turbulence kinetic energy generation due to mean velocity gradient and buoyancy respectively, S_k and S_ε are user defined source term for k and ε respectively, and C_2 , $C_{1\varepsilon}$, and $C_{3\varepsilon}$ are constant.

Constant, $C_{1\varepsilon}$, can be described in Eq. (23);

$$C_{1\varepsilon} = \max \left[0.43, \frac{\eta}{\eta+5} \right], \eta = S \frac{k}{\varepsilon}, S = \sqrt{2S_{ij}S_{ij}} \quad (23)$$

Where η is effectiveness factor, and S_{ij} is mean rate of strain tensor. Realizable k -epsilon model is chosen due to its accuracy by satisfies constraints on Reynolds stresses and consistent with physics of turbulent flows.

2.2 Boundary Conditions and Computational Methods

Figure 1 illustrates the two dimensional (2D) computational domains studied where the domain is a packed sand column. It is assumed the packed sand column is porous media consisting of spherical and uniformed particles size with mean diameter of 150 μm and porosity of 40%. The initial fluid contained within the domain is 40% residual oil to represent as initial residual oil within the reservoir and 60% connate water to represent as irreducible water concentration within the reservoir. It is assumed there is no temperature changes throughout the domain thus no heat transfer occurs within the domain.

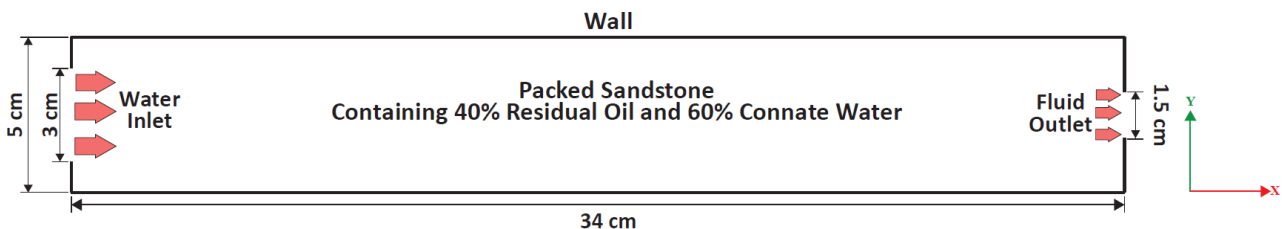


Fig. 1. Computational domain of packed sand column

Fluid Structured Interaction (FSI) is used to simulate and predict the hydrodynamic between the interaction of water, oil, and sand. Using numerical simulation, it able to model all the reservoir conditions such as temperature, pressure, and different forces. Numerical simulation also able to

scales up to real conditions of the reservoirs by using laboratory results where this will decrease the operational risks [20]. In this investigation, ANSYS Fluent is used to predict hydrodynamic flow qualitatively and quantitatively within the sand column (artificial oil reservoir) based on injection rate and oil viscosity parameters that can affect the sweep efficiency of the waterflooding method within the packed sand column.

The operating condition within the domain is atmospheric condition (101.325 kPa) for pressure and 27°C for temperature. In this investigation, injection rate and oil viscosity are the parameters to be studied. Injection rates used in these investigations are 1.0 ml/min (2.357×10^{-5} m/s), 1.5 ml/min (3.537×10^{-5} m/s), 2.0 ml/min (3.333×10^{-5} m/s), 2.5 ml/min (5.894×10^{-5} m/s), 3.0 ml/min (7.074×10^{-5} m/s), and 3.5 ml/min (8.252×10^{-5} m/s). Meanwhile, oil viscosity used in these investigations are 1.0 cP, 2.4 cP, 5.0 cP, 10.0 cP, 15.0 cP, and 20.0 cP. Unsteady state condition is simulated for 1800 seconds. The mesh independent test is performed, and mesh size of 0.005 mm is selected by parameterize the sizing of the meshing of the model and the velocity outlet. Figure 2 shows meshed computational domain with selected mesh size.

The pressure–velocity coupling was solved by SIMPLE algorithm. For the water injection, the inlet boundary condition is velocity inlet while for the outlet boundary condition is pressure outlet. The wall boundary conditions were treated as no slip boundary conditions. The under-relaxation factors for pressure, momentum, turbulence kinetic energy, and turbulence dissipation rate were 0.3, 0.7, 0.8, and 0.8 respectively. The convergence criterion for the residuals was less than 1×10^{-5} for each calculated parameter.

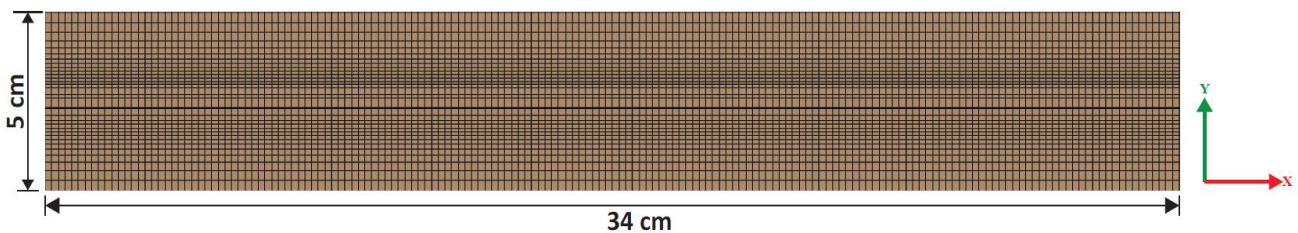


Fig. 2. Meshed computational domain

3. Results and Discussion

3.1 Simulation Validation

Validation is done to determine the accuracy and precision of the certain mathematical model simulation. For this study, validation is done by comparing the viscous fingering occurrence and pattern between one input one outlet Hele-Shaw model experiment done by Kargozarfard *et al.*, [10] and the computational waterflooding simulation results. Figure 3(a) shows the pattern of viscous fingering occur within the Hele-Shaw model for the injection rate of 1.0 ml/min and oil (olein) viscosity of 6.277 cP. Meanwhile, Figure 3(b) and Figure 3(c) show viscous fingering within the porous medium of the waterflooding simulation done with injection rate of 1.0 ml/min and oil viscosity of 5 cP and 10 cP respectively.

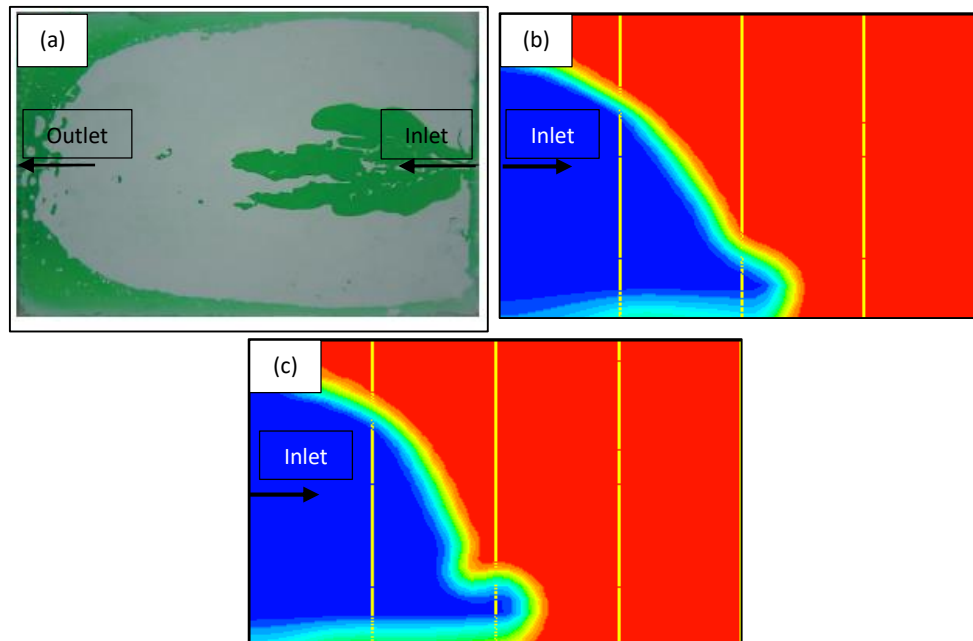


Fig. 3. Distribution of fluids during waterflooding. (a) Hele-Shaw Model Waterflooding by Kargozarfard *et al.*, [10], (b) Waterflooding Simulation for Oil Viscosity 5 cP, (c) Waterflooding Simulation for Oil Viscosity 10 cP

As can be seen in Figure 3(a), the pattern of viscous fingering is slightly different compared to the pattern of viscous fingering seen in Figure 3(b) and Figure 3(c). The length of fingering formed in Figure 3(a) is longer compared to the length of fingering formed in Figure 3(b) and Figure 3(c). This is due to the inlet injected velocity even though the volumetric injection rate is the same, and the oil viscosity is nearly similar. The injected velocity in Figure 3(a) is about 4.331 m/s while injected velocity in Figure 3(b) and Figure 3(c) is about 2.35×10^{-5} m/s which is a very significant difference between both velocities.

Since the injected velocity in Figure 3(a) is higher than Figure 3(b) and Figure 3(c), this can affect the capillary number within the system thus affecting the stability between the fluids interface and the pattern of the fingering formed within the system. Even though, the fingering pattern between Figure 3(a), Figure 3(b) and Figure 3(c) are different, the computational simulation done is considered acceptable since it is able to simulate the viscous fingering occurrence within the system for the oil viscosity of 5 cP and 10 cP as seen in Figure 3(b) and Figure 3(c) respectively which is within the range of oil viscosity of 6.277 cP used in experimental.

3.2 Effect of Injection Rate and Oil Viscosity on Viscous Fingering

Displacement of residual oil of various oil viscosity within porous medium has been investigated. Water is used as displacing fluid with different injection rates to show the effect of injection rate towards the displacement of residual oil with various oil viscosity. Figure 3 to Figure 8 show the displacement of various oil viscosity with injection rates of 1.0 ml/min, 1.5 ml/min, 2.0 ml/min, 2.5 ml/min, 3.0 ml/min, and 3.5 ml/min respectively. Meanwhile, correlation between mobility ratio and viscous fingering can be seen in Figure 9 and Figure 10 based on viscosity ratio parameter.

As can be seen from Figure 4, there is no fingering occurred during the displacement for oil viscosity 1 cP to 5 cP. As the oil viscosity increases, the distance of displacement decreases. The decrease in distance can be seen from 6 cm, 5.5 cm, to 4.8 cm from the leading edge for 1 cP, 2.4 cP, and 5 cP respectively. Meanwhile, for oil viscosity of 10 cP, 15 cP, and 20 cP, the displacement

distance observed at the distance of 4.8 cm. The fingering observed within the porous medium too. It can be seen from Figure 4 that for oil viscosity 1 cP, 2.4 cP and 5 cP, with injection rate of 1.5 ml/min, the displacement distance are 7.5 cm, 7.0 cm, and 6.5 cm respectively with no fingering observed. Meanwhile, the fingering can be observed with displacement distance of 6.5 cm for oil viscosity of 10 cP, 15 cP, and 20 cP as in Figure 5.

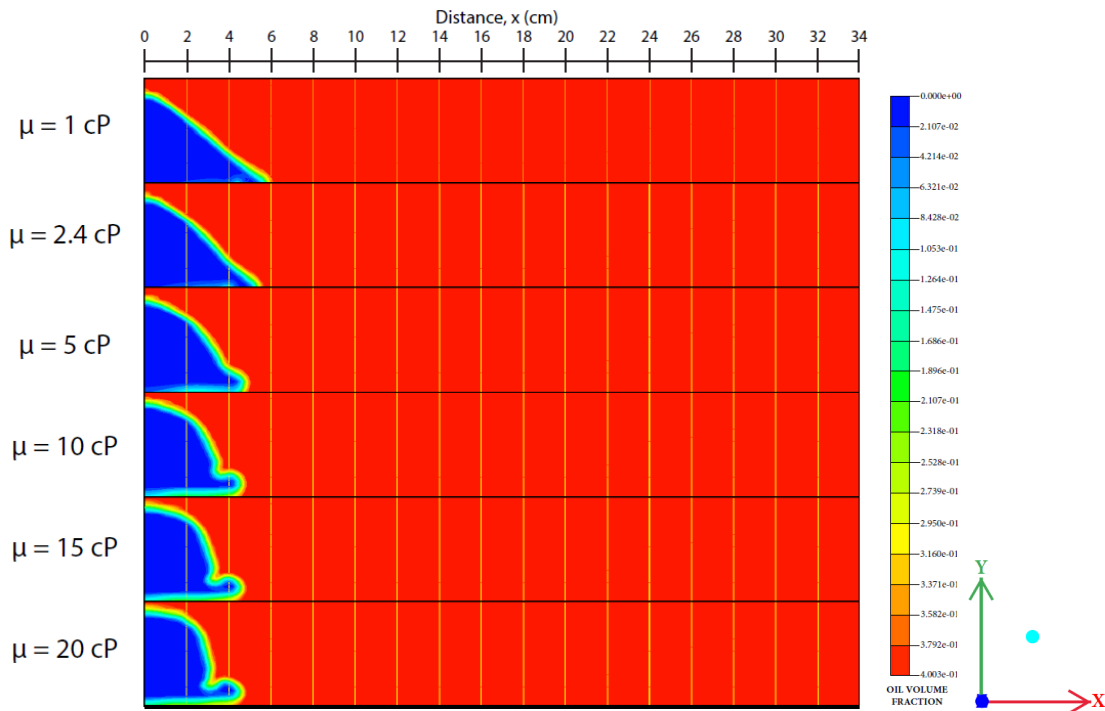


Fig. 4. Displacement of various oil viscosity with injection rate of 1.0 ml/min

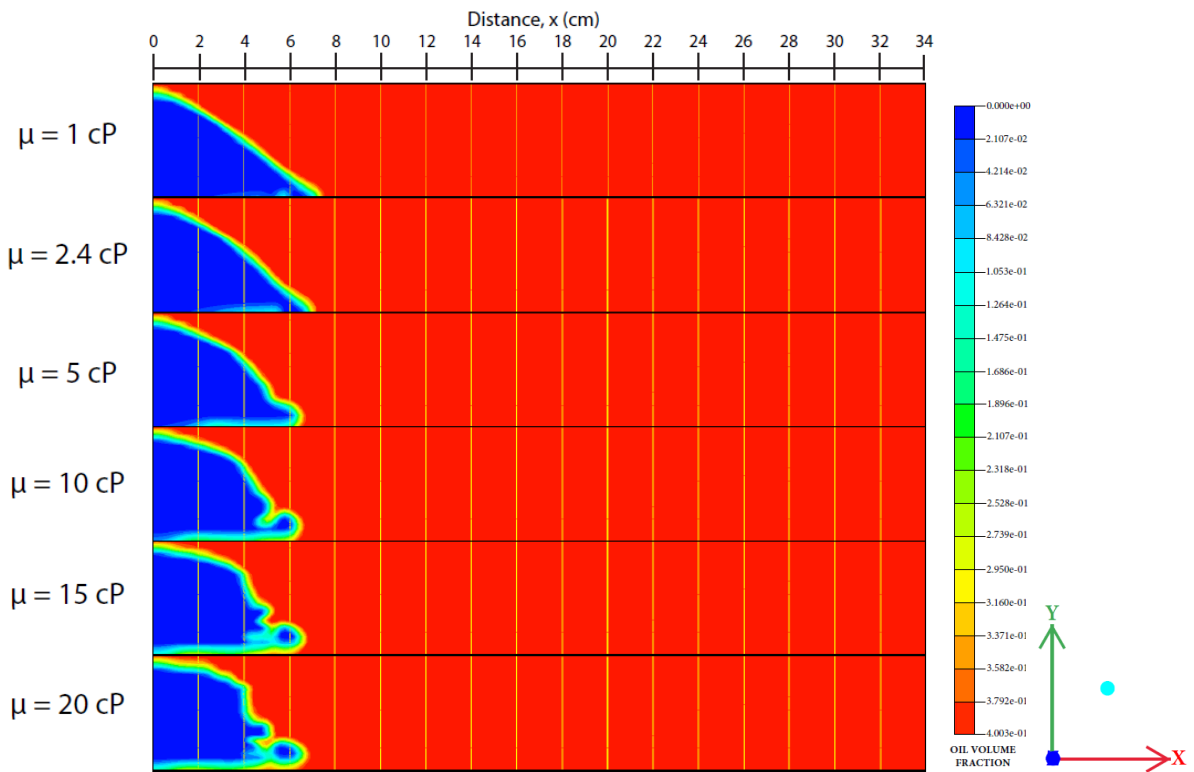


Fig. 5. Displacement of various oil viscosity with injection rate of 1.5 ml/min

There is no fingering observed for oil viscosity of 1 cP, 2.4 cP and 5 cP during waterflooding of injection rate of 2.0 ml/min as illustrated in Figure 6. All three oil viscosities have displacement distance of 8.8 cm, 8.5 cm, and 8.0 cm respectively. Meanwhile, for oil viscosity of 10 cP, 15 cP, and 20 cP, fingering is observed for each oil viscosity with displacement distance of 8.2 cm, 8.5 cm, and 9.0 cm respectively. As can be seen in Figure 7, no fingering observed for oil viscosity of 1 cP and 2.4 cP. Both oil viscosity has displacement distance of 10 cm. Meanwhile, for oil viscosity 5 cP, it has displacement distance of 9.8 cm with minimal viscous fingering start to form. As can be seen in Figure 6, for oil viscosity of 10 cP, 15 cP, and 20 cP, the displacement distance of 9.8 cm, 10 cm, and 10.2 cm respectively with more than one fingering can be observed.

As can be seen in Figure 8, there is no fingering observed for oil viscosity of 1 cP and 2.4 cP and both oil viscosities have displacement distance of 11 cm. Meanwhile, for oil viscosity of 5 cP, 10 cP, 15 cP, and 20 cP, there are fingering can be observed within the porous medium with only minimal fingering formed for oil viscosity of 5 cP. For displacement distance, oil viscosity of 5 cP, 10 cP, 15 cP, and 20 cP have 11 cm, 12 cm, 11.8 cm, and 12.2 cm respectively. For displacement contour of injection rate 3.5 ml/min which can be seen in Figure 9, the displacement distance for 1 cP and 2.4 cP is 12.2 for both oil viscosity with no viscous fingering observed. Meanwhile, for oil viscosity of 5 cP, 10 cP, 15 cP, and 20 cP, the displacement distance is 12.2 cm, 13.8 cm, 14.2 cm and 15 cm respectively. Minimal viscous fingering can be observed for oil viscosity 5 cP whereas numbers of fingering are observed for oil viscosity of 10 cP, 15 cP, and 20 cP.

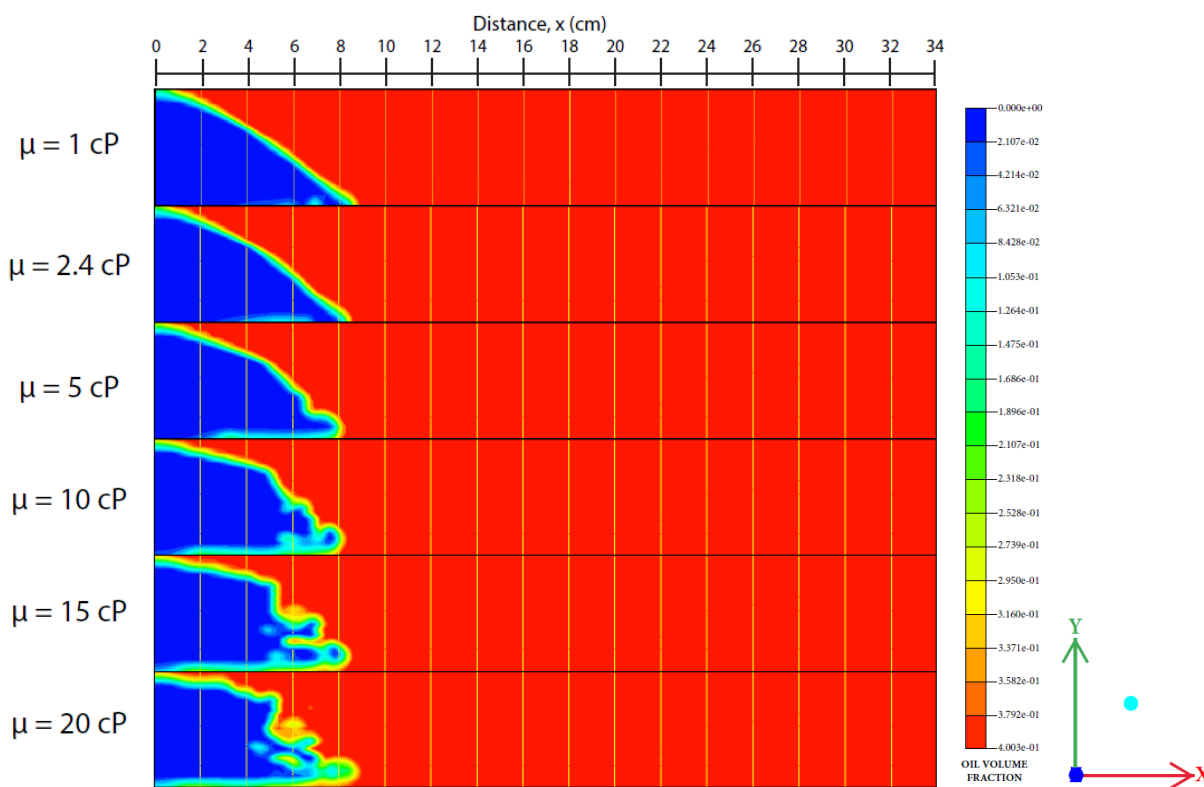


Fig. 6. Displacement of various oil viscosity with injection rate of 2.0 ml/min

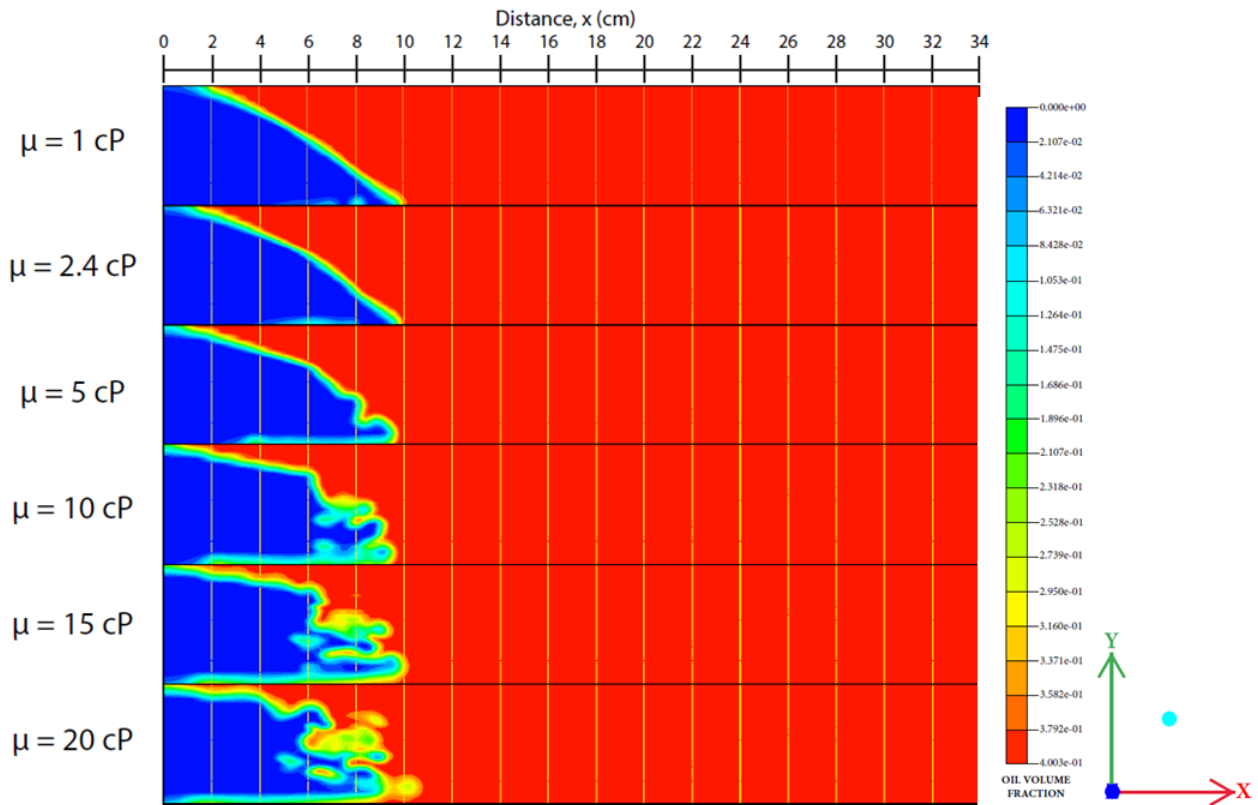


Fig. 7. Displacement of various oil viscosity with injection rate of 2.5 ml/min

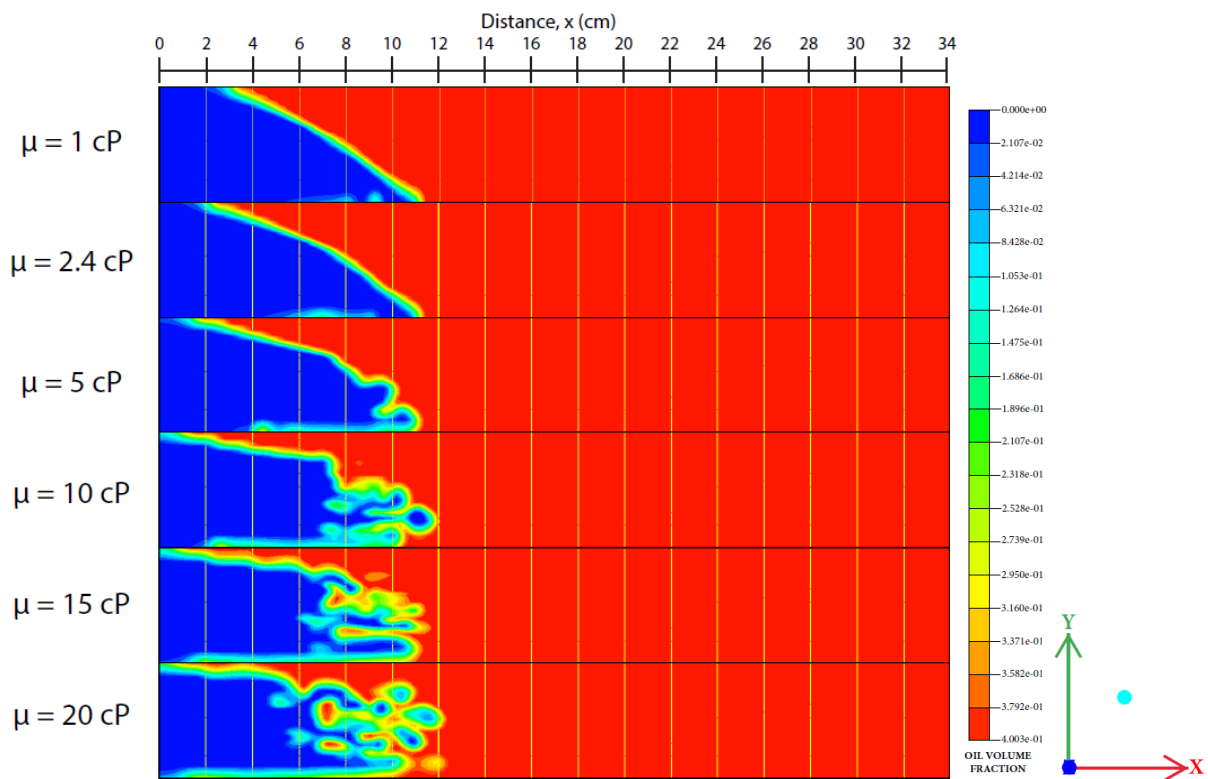


Fig. 8. Displacement of various oil viscosity with injection rate of 3.0 ml/min

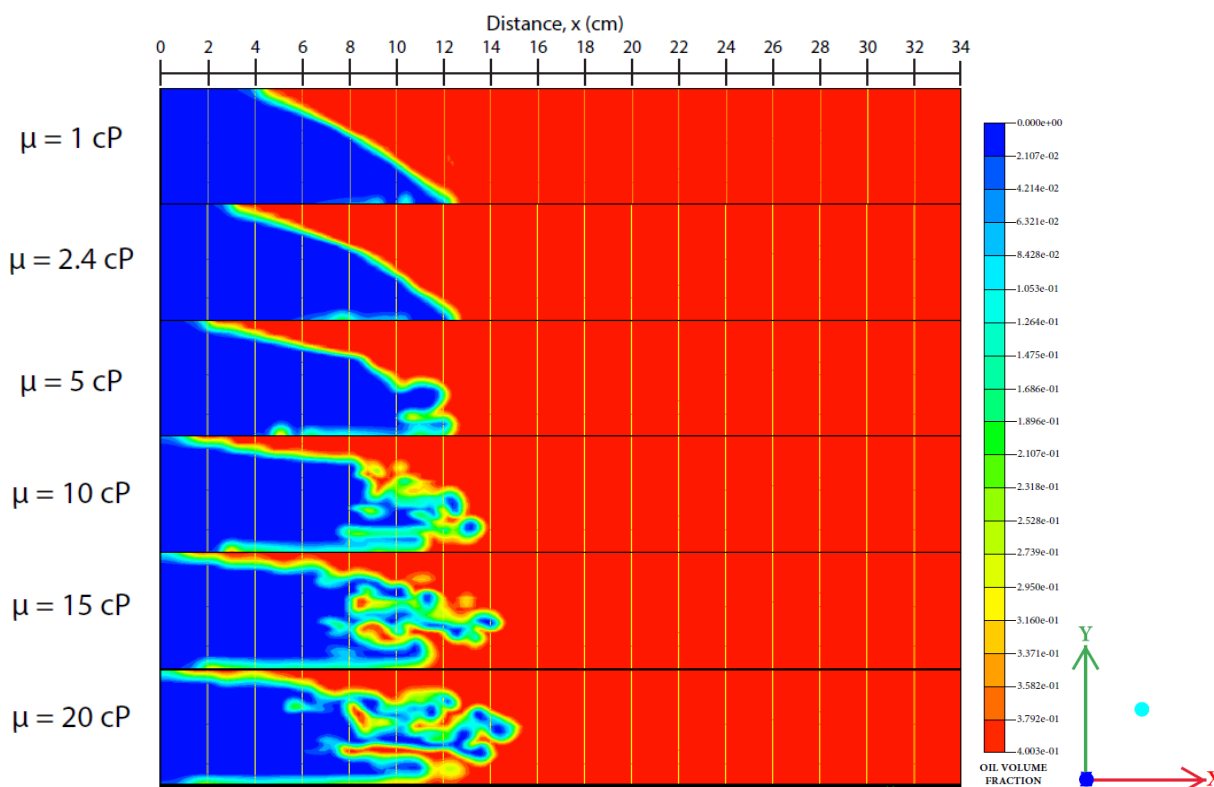


Fig. 9. Displacement of various oil viscosity with injection rate of 3.5 ml/min

Generally, as can be seen from Figure 4 to Figure 9, as injection rate increase, the displacement distance also increases. It also can be seen as injection rate increase; viscous fingering has more tendency to form within the porous medium as the oil viscosity increase. Consider Figure 9 for the case of oil viscosity 20 cP, the longest displacement distance compared to other oil viscosity for various injection rate. It can be observed there is fractional residual oil behind waterflood front (at point 8 cm to 14 cm) even though the waterflood front already advance to 15 cm. This is due to viscous fingering. The observation made for oil viscosity of 1 cP and 2.4 cP illustrates no viscous fingering for all injection rates. This phenomenon is expected since the minimal or nonexistence of residual oil behind the waterflood front. This observation agrees with study done by Suekane *et al.*, [19] who concluded that viscous fingering could affect the waterflooding efficiency.

Viscous fingering commonly occurred due to different fluid properties between displacing fluid and displaced fluid. As stated by Homsy [21], physical properties such as viscosity, density, gravity, and surface tension can cause viscous fingering formation. Pressure forces from flow velocity on the displaced fluid cause displacement of the interface. Any positive net pressure force can amplify the displacement leading to an instability when there are sudden changes in the fluid physical properties such as viscosity. It has been evidenced in current study, instability is caused by gravitational and viscosity forces for horizontal displacement. Also, viscosity ratio which is measured between displacing fluid and displaced fluid is the main factor of viscous fingering formation.

The injection rate is also another parameter causing the viscous fingering formation. The current study has showed the increment in the injection rate causing the interface between fluids to become unstable. Instability number (Eq. (8)) where viscosity ratio incorporates with capillary number is used to determine flow stability pattern for heavy oil waterflooding. The instability number for this study are ranging in the order of 103 to 106 which is more than the order of 103. This indicates the flow within the porous medium is unstable thus forming viscous fingering when injection rate and viscosity

ratio increased. Consequently, show that both viscosity ratio and injection rate are the main factors of viscous fingering formation. This is also in agreement with Kargozarfard *et al.*, [10].

3.3 Effect of Viscosity Ratio and Relative Permeability Ratio on Mobility Ratio

Figure 10 shows mobility ratio for various injection rate and oil viscosity. As can be seen in Figure 10, oil viscosity 1 cP has the lowest mobility ratio regardless the injection rate. Meanwhile, oil viscosity 20 cP has the highest mobility ratio for all injection rates. From Figure 10, it is observed oil viscosity of 15 cP and 20 cP has mobility ratio more than unity starting from injection rate of 2.5 ml/min and 1.5 ml/min respectively. Figure 11 shows the relationship between viscosity ratio and mobility ratio where it is observed that mobility ratio is directly proportional to viscosity ratio. As can be seen from Figure 11, as viscosity ratio increase, the mobility ratio also increases for the same injection rate.

Viscosity ratio is one of factor affecting mobility ratio as per Eq. (2). Viscosity ratio also can affect the viscosity fingering formation in porous medium. As observed from Figure 11, as viscosity ratio increase, mobility ratio also increases. Since the viscosity ratio increases, viscous fingering occurred within the porous medium. It shows the relationship where the viscosity ratio increment leads to high mobility ratio and causing poor displacement within the porous medium. Furthermore, viscosity ratio has major impact on mobility ratio. This also support the statement of mobility ratio more than unity is unfavourable by taking an example from oil viscosity 20 cP in Figure 9 where there is fractional residual oil behind waterflood front which display poor displacement because the effect of viscous fingering in the porous medium.

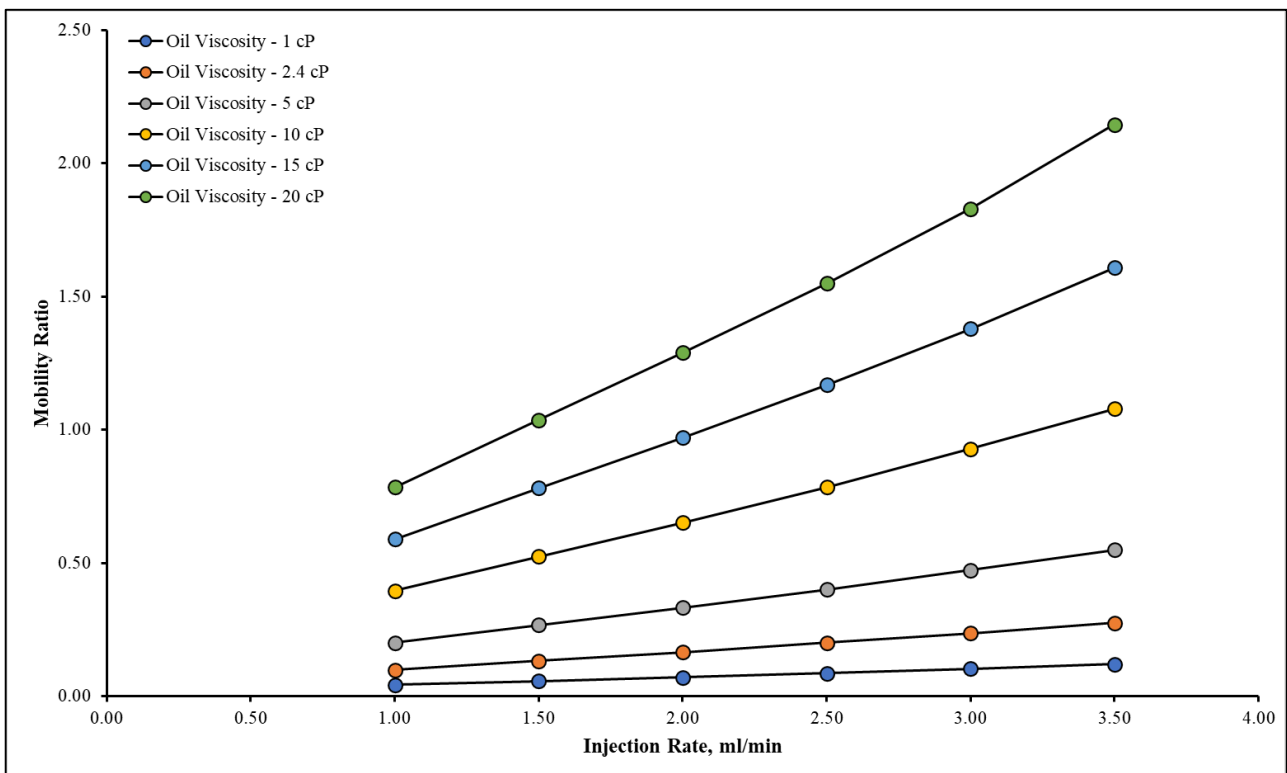


Fig. 10. Effect of Injection Rate on Mobility Ratio for Various Oil Viscosity

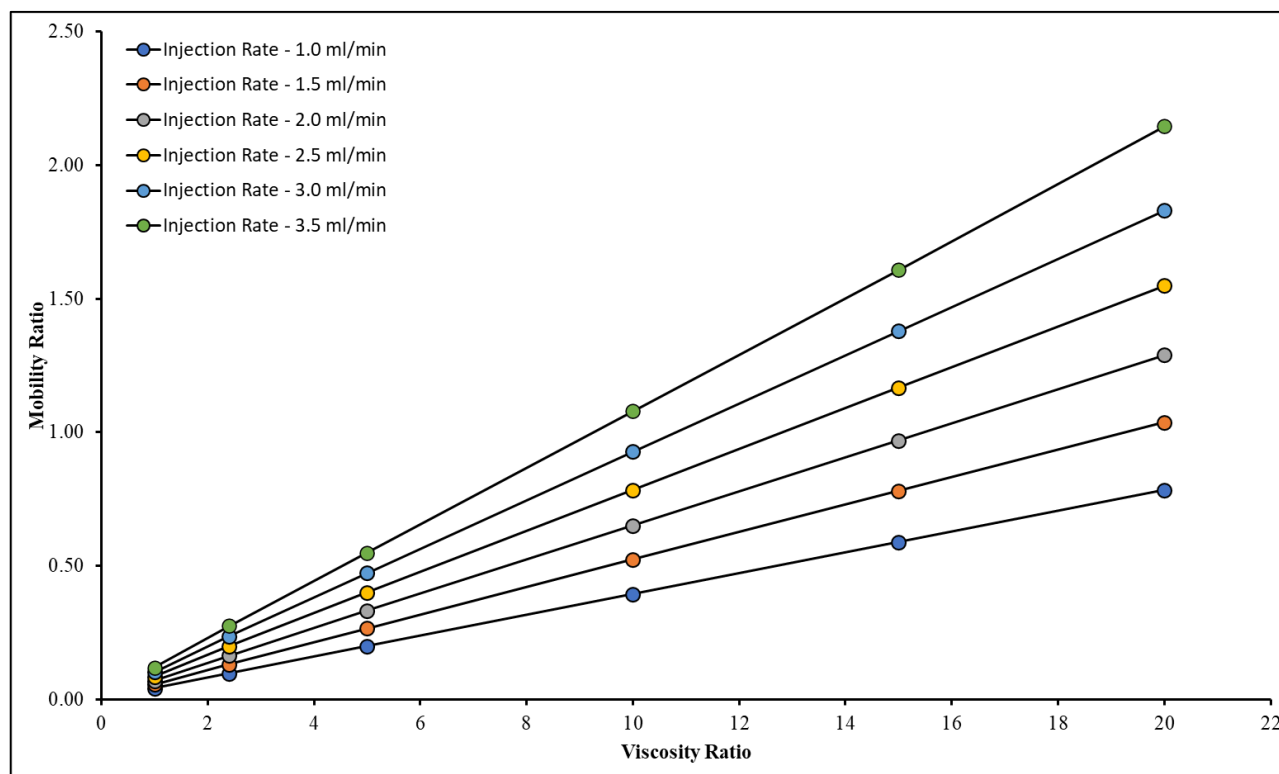


Fig. 11. Effect of Viscosity Ratio on Mobility Ratio for Various Injection Rate

Permeability in a reservoir is a measurement on amount of fluid can flow through a rock or porous medium under a specified pressure drop. Therefore, permeability is a physical property of the rock, and it means absolute permeability of a rock or porous medium is constant. Relative permeability is a concept used to express the reduction in flow capability due to the presence of multiple mobile fluids. Several factors affecting relative permeability are the pore geometry, wettability, fluid distribution, and fluid saturation. Relative permeability ratio (k_{rw}/k_{ro}) in mobility ratio is calculated at connate water saturation, S_{wc} , for relative permeability to oil, k_{ro} , and at residual oil saturation, S_{or} , for relative permeability to water, k_{rw} .

Figure 12 shows the relationship between relative permeability ratio on mobility ratio for various set data of injection rate and oil viscosity. It can be observed the relative permeability is directly proportional with the mobility ratio. It also can be observed as injection rate increase, the relative permeability ratio also increases. As injection rate of water increase, it will increase the water saturation within porous medium. As water saturation increases, the amount of water capable to mobilize to be found. Therefore, the fraction occupied by water in the pore volume also increased. The relative permeability is found to be related on the ability of fluid to occupy a fraction of the total pore volume [22]. Therefore, the phenomenon directly causing the relative permeability increases when the water saturation increase.

Meanwhile, it can be observed from Figure 12, when the oil viscosity increases, the relative permeability ratio is decreased. This is due to the viscous force dominate the capillary force. When viscosity increases, it can cause the injected water unable to flow smoothly within the porous medium. Consequently, this causes the water saturation decrease when the viscosity increases even though the injection rate increase. Thus, causing the relative permeability also to decrease. This also has been reported by study done by Domínguez and Moreno [23] where the relative permeability curve is dependence on injection rate and viscosity. This shows the important role of injection rate

and oil viscosity towards relative permeability. Consequently, the phenomenon affects the mobility ratio.

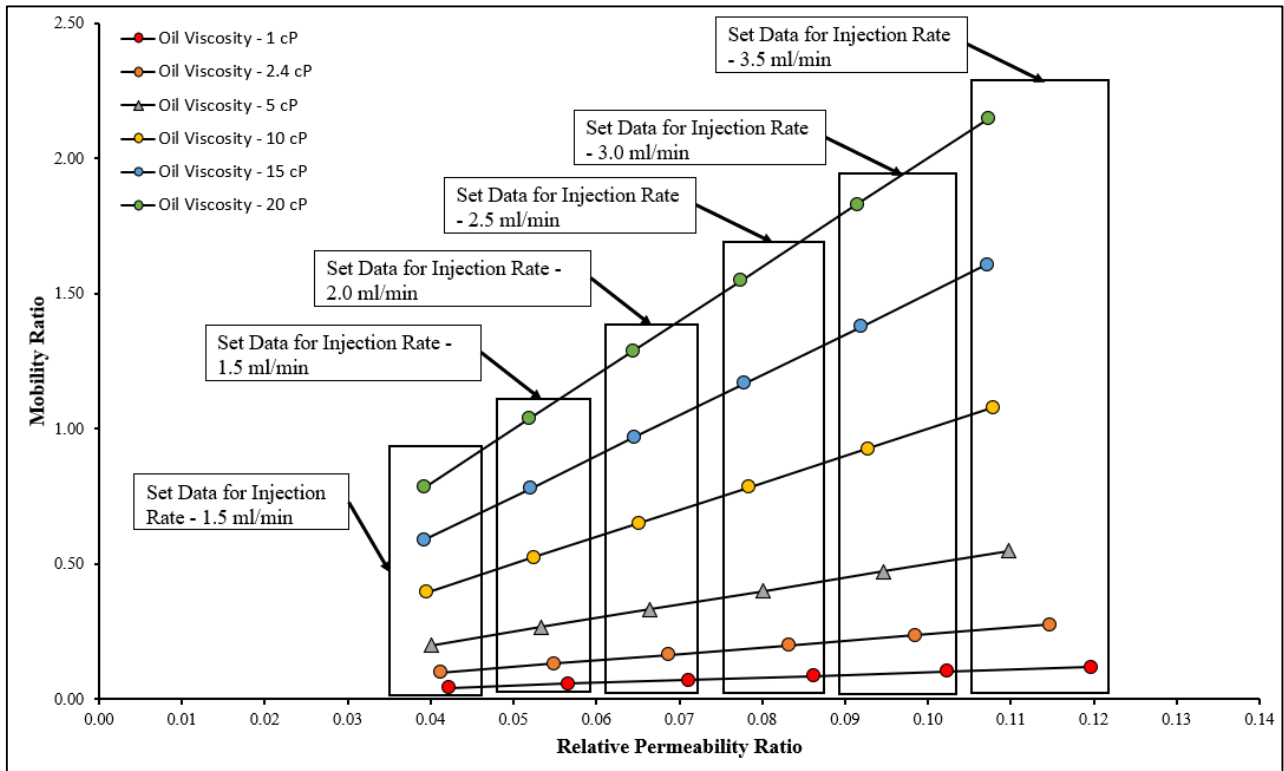


Fig. 12. Effect of Relative Permeability Ratio on Mobility Ratio for Various Injection Rate

3.4 Effect of Mobility Ratio on Sweep Efficiency

Figure 13 shows the relationship between mobility ratio and sweep efficiency. Generally, as can be observed in Figure 13, mobility ratio is directly proportional with sweep efficiency. As can be seen in Figure 13, as injection rate increase, the sweep efficiency also increases and injection rate of 3.5 ml/min has the highest sweep efficiency for all oil viscosity. Meanwhile, injection rate of 1.0 ml/min has the lowest sweep efficiency for all oil viscosity. In term of oil viscosity, the highest sweep efficiency is on oil viscosity of 1 cP and the lowest sweep efficiency is on 20 cP for all injection rates. This concludes for same injection rate, as mobility ratio increases, the sweep efficiency decreased. This is due to the increasing of oil viscosity which can affect the injected water flow in the porous medium.

The capillary forces increase when injection rate increase leading to proper oil displacement thus giving high injection rate has high sweep efficiency. The capillary forces are also dominated by the viscous force as oil viscosity increased from 1 cP to 20 cP affecting the oil displacement in the porous medium even though at high injection rate ranging from 1.0 ml/min to 3.5 ml/min. Conclusively, the mobility ratio affect the sweep efficiency through the injection rate and oil viscosity.

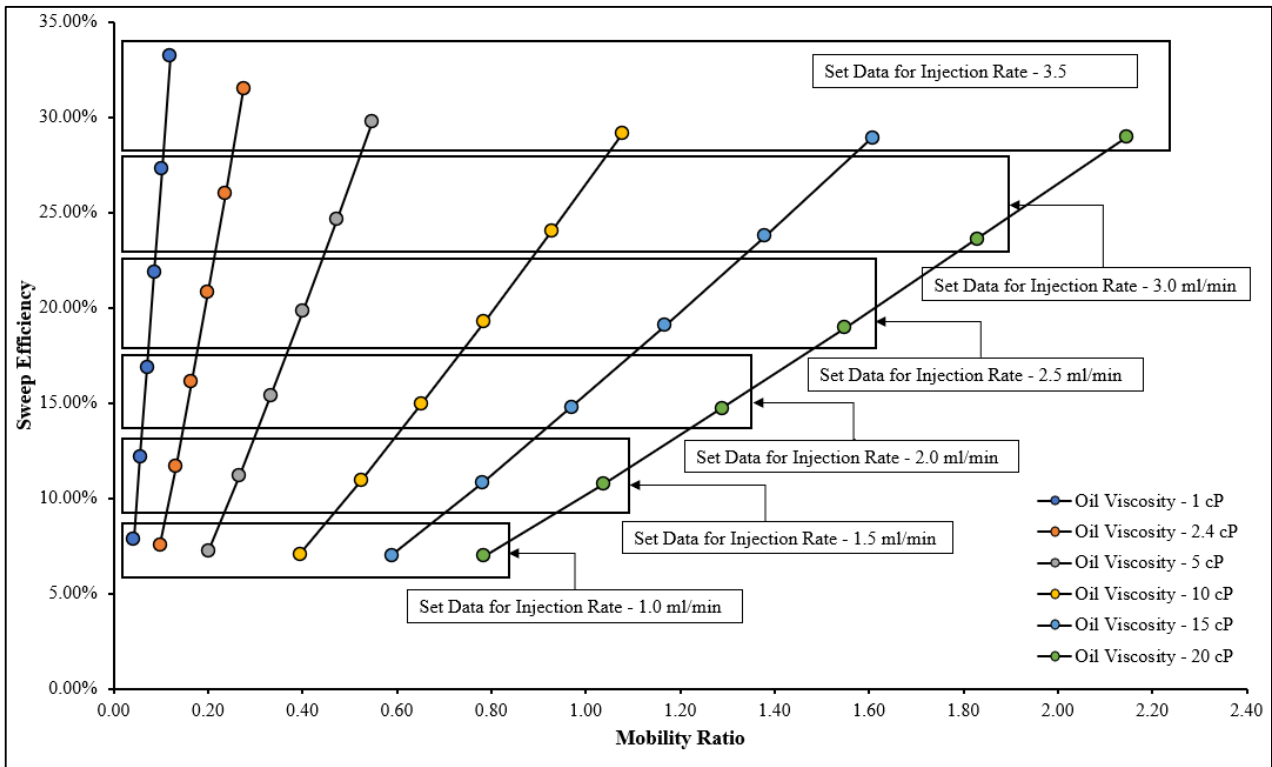


Fig. 13. Effect of Mobility Ratio on Sweep Efficiency

4. Conclusions

As conclusion, both injection rate and oil viscosity play a major role for oil recovery process affecting both viscous forces and capillary forces. The injection rate of 1.0 ml/min and 1.5 ml/min found to be best fitted injection rate for all oil viscosity. It has been observed no or minimal viscous fingering that occurred within the sand column for both injection rates. Viscous fingering is to be avoided during oil recovery process since it affects oil recovery performance. It can be concluded high injection rate for high oil viscosity causing viscosity fingering formation.

The injection rate and oil viscosity also affect the mobility ratio and sweep efficiency. The increased in the injection rate and oil viscosity affect directly proportional to the mobility ratio. The mobility ratio more than unity is not preferable for waterflooding process causing viscous fingering within the sand column. Eventually, this is affecting sweep efficiency. High injection rate has the high sweep efficiency. However, high oil viscosity can cause sweep efficiency to decrease. This is due to the increment of mobility ratio thus causing viscous fingering to occur. Therefore, a suitable injection rate needs to be determined either for light or heavy oil recovery to avoid or minimize the viscous fingering formation within the reservoir.

Acknowledgement

This research was funded by a grant from Ministry of Science, Technology, and Innovation of Malaysia (MOSTI) (FRGS Grant No: FRGS/1/2018/TK07/MOSTI/02/3). The author would like to acknowledge excellent programming assistance from Assoc. Prof. Ir. Dr. Nadiahnor Md. Yusop and Dr. Noraishah Othman. Thank you also to Universiti Teknologi MARA (UiTM) and Agensi Nuklear Malaysia for the guidance and support.

References

- [1] Rahman, Musfika, and Iskandar Dzulkarnain. "RSM for Modelling the CO2 Effect in the Interfacial Tension Between Brine and Waxy Dulang Crude Oil During LSW-WAG EOR." *Journal of Advanced Research in Fluid Mechanics and Thermal Sciences* 85, no. 2 (2021): 159-174. <https://doi.org/10.37934/arfmts.85.2.159174>
- [2] Nayan, Asmahani, Nur Izzatie Farhana Ahmad Fauzan, Mohd Rijal Ilias, Shahida Farhan Zakaria, and Noor Hafizah Zainal Aznam. "Aligned Magnetohydrodynamics (MHD) Flow of Hybrid Nanofluid Over a Vertical Plate Through Porous Medium." *Journal of Advanced Research in Fluid Mechanics and Thermal Sciences* 92, no. 1 (2022): 51-64. <https://doi.org/10.37934/arfmts.92.1.5164>
- [3] Miller, Richard J. "Petroleum Economics." In *Standard Handbook of Petroleum and Natural Gas Engineering*, pp. 985-1033. Gulf Professional Publishing, 1996. <https://doi.org/10.1016/B978-088415643-7/50011-X>
- [4] Green, Don W., and G. Paul Willhite. *Enhanced oil recovery*. Vol. 6. Richardson, TX: Henry L. Doherty Memorial Fund of AIME, Society of Petroleum Engineers, 1998.
- [5] Eremin, Nikolai A., and Larisa N. Nazarova. *Enhanced Oil Recovery Methods*. Russian State University of Oil and Gas (2001).
- [6] Muggeridge, Ann, Andrew Cockin, Kevin Webb, Harry Frampton, Ian Collins, Tim Moulds, and Peter Salino. "Recovery rates, enhanced oil recovery and technological limits." *Philosophical Transactions of the Royal Society A: Mathematical, Physical and Engineering Sciences* 372, no. 2006 (2014): 20120320. <https://doi.org/10.1098/rsta.2012.0320>
- [7] Dugstad, Ø., S. Viig, B. Krognes, R. Kleven, and O. Huseby. "Tracer monitoring of enhanced oil recovery projects." In *EPJ Web of Conferences*, vol. 50, p. 02002. EDP Sciences, 2013. <https://doi.org/10.1051/epiconf/20135002002>
- [8] Pei, Haihua, Guicai Zhang, Jijiang Ge, Mingchao Ma, Lei Zhang, and Yueliang Liu. "Improvement of sweep efficiency by alkaline flooding for heavy oil reservoirs." *Journal of Dispersion Science and Technology* 34, no. 11 (2013): 1548-1556. <https://doi.org/10.1080/01932691.2012.752331>
- [9] Palsson, Bjarni, D. R. Davies, A. C. Todd, and J. M. Somerville. "The water injection process: a technical and economic integrated approach." *Chemical Engineering Research and Design* 81, no. 3 (2003): 333-341. <https://doi.org/10.1205/02638760360596883>
- [10] Kargozarfard, Zahra, Masoud Riazi, and Shahab Ayatollahi. "Viscous fingering and its effect on areal sweep efficiency during waterflooding: an experimental study." *Petroleum Science* 16, no. 1 (2019): 105-116. <https://doi.org/10.1007/s12182-018-0258-6>
- [11] Satter, Abdus, and Ghulam M. Iqbal. "16-Waterflooding and waterflood surveillance." *Reservoir Engineering* (2016): 289-312. <https://doi.org/10.1016/B978-0-12-800219-3.00016-4>
- [12] Groenenboom, Jeroen, Sau-Wai Wong, Tor Meling, Robert Zschuppe, and Brett Davidson. "Pulsed water injection during waterflooding." In *SPE International Improved Oil Recovery Conference in Asia Pacific*. OnePetro, 2003. <https://doi.org/10.2118/84856-MS>
- [13] Fu-qing, Yuan, and Li Zhen-quan. "An Easy Calculation Method on Sweep efficiency of Chemical Flooding." *Applied Mechanics and Materials* 275-277 (2013): 496-501. <https://doi.org/10.4028/www.scientific.net/AMM.275-277.496>
- [14] Gang, H. U. "A new method for calculating volumetric sweep efficiency in a water-flooding oilfield." *Petroleum Exploration and Development* 40, no. 1 (2013): 111-114. [https://doi.org/10.1016/S1876-3804\(13\)60011-7](https://doi.org/10.1016/S1876-3804(13)60011-7)
- [15] Ahmed, Tarek. *Reservoir engineering handbook*. Gulf Professional Publishing, 2018.
- [16] Mamudu, Abbas, Olafuyi Olalekan, and Giegbefumwen Peter Uyi. "Analytical study of viscosity effects on waterflooding performance to predict oil recovery in a linear system." *Journal of Petroleum & Environmental Biotechnology* 6, no. 3 (2015): 221. <https://doi.org/10.4172/2157-7463.1000221>
- [17] Schön, J. H. "Pore space properties." In *Handbook of Petroleum Exploration and Production*, vol. 8, pp. 17-73. Elsevier, 2011. [https://doi.org/10.1016/S1567-8032\(11\)08002-5](https://doi.org/10.1016/S1567-8032(11)08002-5)
- [18] Jin, Fa-Yang, Song Wang, Wan-Fen Pu, Xue-Li Liu, Cheng-Dong Yuan, Shuai Zhao, Yan-Li Tang, and Lian Dou. "The effects of interfacial tension, injection rate, and permeability on oil recovery in dilute surfactant flooding." *Petroleum Science and Technology* 34, no. 16 (2016): 1490-1495. <https://doi.org/10.1080/10916466.2016.1208228>
- [19] Suekane, Tetsuya, Tomotaka Koe, and Pablo Marin Barbancho. "Three-dimensional interaction of viscous fingering and gravitational segregation in porous media." *Fluids* 4, no. 3 (2019): 130. <https://doi.org/10.3390/fluids4030130>
- [20] Jafari, Arezou, Mohammadreza Hasani, Mostafa Hosseini, and Reza Gharibshahi. "Application of CFD technique to simulate enhanced oil recovery processes: current status and future opportunities." *Petroleum Science* 17, no. 2 (2020): 434-456. <https://doi.org/10.1007/s12182-019-00363-7>
- [21] Homsy, George M. "Viscous fingering in porous media." *Annual Review of Fluid Mechanics* 19, no. 1 (1987): 271-311. <https://doi.org/10.1146/annurev.fl.19.010187.001415>

- [22] Archer, J. S., and C. G. Wall. "Relative Permeability and Multiphase Flow in Porous Media." In *Petroleum Engineering*, pp. 102-121. Springer, Dordrecht, 1986. https://doi.org/10.1007/978-94-010-9601-0_7
- [23] Domínguez, L. G., and R. B. Z. L. Moreno. "Flow Rate Influence in Relative Permeability Curves: Dependence with Oil Viscosity." *International Journal of Engineering & Technology IJET-IJENS* 16, no. 1 (2016).
- [24] Mai, A., and A. Kantzas. "Heavy oil waterflooding: effects of flow rate and oil viscosity." *Journal of Canadian Petroleum Technology* 48, no. 03 (2009): 42-51. <https://doi.org/10.2118/09-03-42>
- [25] Doorwar, Shashvat, and Kishore K. Mohanty. "Viscous-fingering function for unstable immiscible flows." *SPE Journal* 22, no. 01 (2017): 19-31. <https://doi.org/10.2118/173290-PA>
- [26] Sorbie, K. S., A. Y. Al Ghafri, Arne Skauge, and E. J. Mackay. "On the modelling of immiscible viscous fingering in two-phase flow in porous media." *Transport in Porous Media* 135, no. 2 (2020): 331-359. <https://doi.org/10.1007/s11242-020-01479-w>